

Chapter 4 Results and Discussion

4.1 Carbon Nanotubes *In Situ* Grown on Silicon by Using HWCVD

A simplified Chemical Vapor Deposition method is described for *in situ* synthesis of multiwalled carbon nanotubes. The synthesis apparatus is similar to that used to deposit CVD diamond. However, an Fe-Cr wire is selected and coiled as the filament to grow nanotubes. The tubes grow because the filament acts as both a heat source for pyrolysis, and a source of metal for the catalyst. The evaporated metal atoms can be considered to catalyze the growth of carbon nanotubes. The system has the potential to inexpensively synthesize large amounts of nanotubes continuously by combining physical and chemical vapor deposition.

4.1.1 Background

Several methods were reported for growing CNTs *in situ* without pre-deposition of a catalyst layer. One such method provides catalysts from the vapor source containing the metal element [26], while another uses the reactant gas which can act as a catalyst in certain substrates [27,28]. However, almost all methods use chemical means to produce a catalyst *in situ*; few employ physical vapor deposition (PVD) to produce such a catalyst. CNTs were deposited as a by-product of diamond thick films in a hot filament CVD (HFCVD) system while copper was evaporated *in situ* from copper-covered parts near hot filaments to act as a catalyst during deposition [29]. However, this method seems to be an impractical means of synthesizing CNTs. In this study, we report a simple, nontoxic, inexpensive *in situ* HWCVD method for preparing multiwalled nanotubes (MWCNTs) on silicon. The method uses the wire as the heat source for pyrolysis, and the catalytic evaporation of the Fe-Cr wire.

4.1.2 Characterization of Carbon Nanotubes

SEM images in Fig. 21 show the surface morphology of the CNTs. A random tube network including curved tubes was formed. Tubes were about 60-80 nm in diameter and a few tens of microns long. The location of CNTs on the sample was investigated using the SEM images. The black images reveal that most of the CNTs were under the lowest position of the coiled Fe-Cr wire. TEM analysis of the CNTs was performed to confirm that these structures are truly CNTs, and not carbon fibers. Figure 22 shows a representative TEM micrograph of the nanotubes. A comparison of our result with images presented elsewhere [27,29] shows that these tubes are multiwalled CNTs. The darker nanotube walls indicate that the nanotubes are multiwalled and hollow rather than solid fibers. The bending and twisting defects of the CNTs shown in Fig. 22 are consistent with the SEM images in Fig. 21. TEM image also shows that the CNTs have inner diameters of around 20 nm.

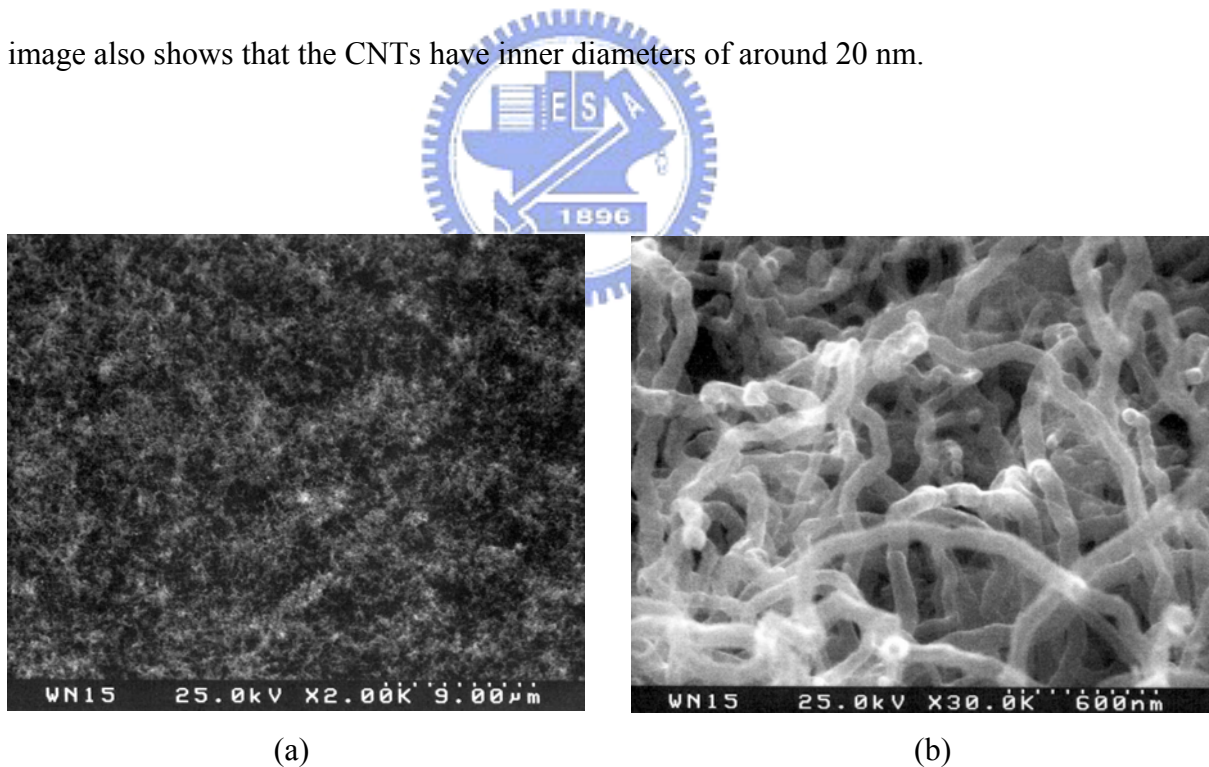


Fig. 21. SEM images of CNTs on silicon, obtained with 15 sccm CO₂ carrier gas; (a) scale bar is 9 μm, and (b) scale bar is 600 nm.



Fig. 22. TEM image of the multiwalled CNTs, obtained with 15 sccm CO₂ carrier gas.

Figure 23 displays the Raman spectrum of CNTs grown by direct HWCVD. Below 3500 cm⁻¹, the spectrum shows four strong peaks at 1350 (D line), 1582 (G line), 2691, and 2940 cm⁻¹, a weak peak at 3230 cm⁻¹, and a weak peak at ~1615 cm⁻¹ (D' line) associated with the line at 3230 cm⁻¹ [157]. While the peak position and shape depended slightly on the location measured, Fig. 23 presents the main features of the spectra, which agree with those observed by other groups [25,157]. A comparable intensity of the G and D lines implies a high density of structural defects in the curved graphene sheets [158]. The SEM and TEM images of the CNTs in this study reveal that the CNTs contain carbon nanoparticles. The appearance of the strong D line can be interpreted as representing a large number of crystalline domains on the nanometer scale, enhanced by the surfaces of the tubes [157].

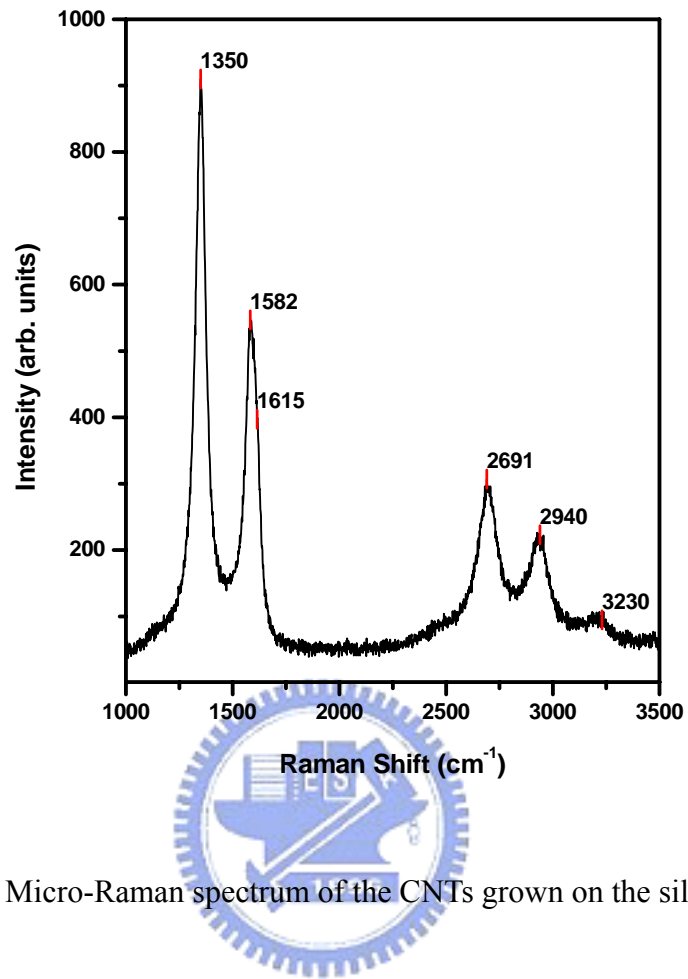
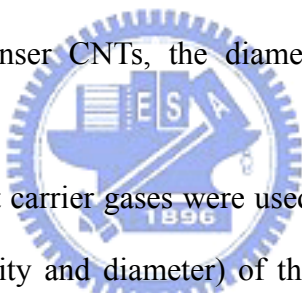


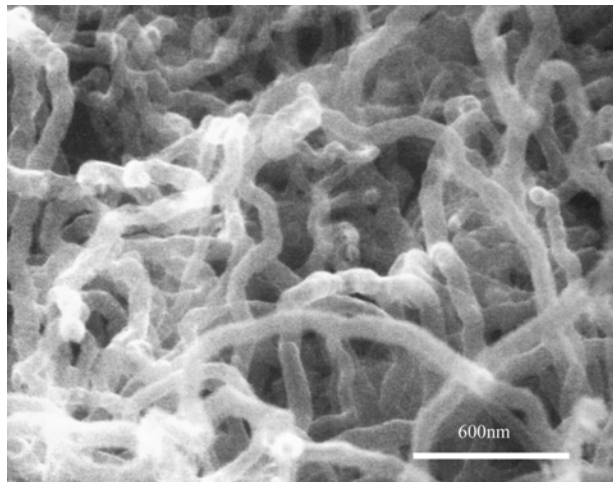
Fig. 23. Micro-Raman spectrum of the CNTs grown on the silicon wafer.

4.1.3 Effect of Carrier Gases and Flow Rate on Growth of CNTs

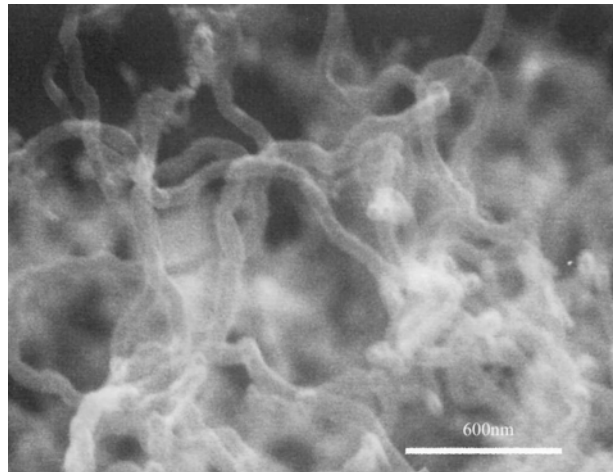
The location of CNTs on the sample was examined using SEM. The black images show reveal that most CNTs were under the lowest position of the coiled Fe-Cr wire. Figures 24 and 25 display the SEM pictures of CNTs grown with different carrier gases. Figure 24 shows the surface morphology of the CNTs, growing on silicon with various CO₂ flow rates. A lower flow rate results in denser CNTs, but the diameter of these CNTs decrease as flow rate increases. These SEM images also show that a random tube network, including curved tubes, was formed. Furthermore, Fig. 24 shows that many fewer CNTs are yielded at a higher flow rate. Therefore, a higher flow rate cannot guarantee the growth of more CNTs. Hence, a lower flow rate is preferable in forming CNTs films, with respect to production yield. Figure 25 displays SEM images of CNTs, growing on silicon with various Ar flow rates. As for CO₂, a lower flow rate results in denser CNTs, the diameter of which decreases as flow rate increases.



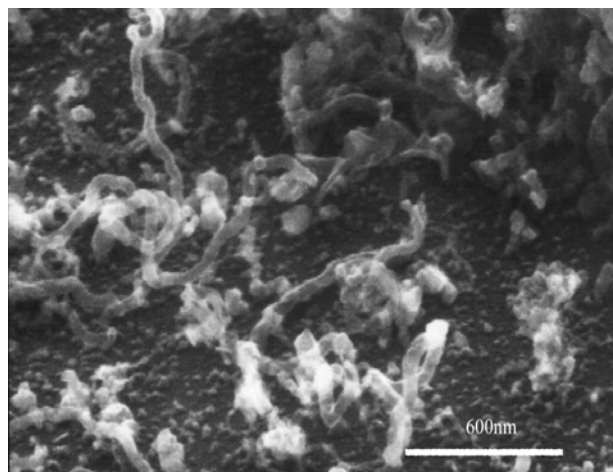
In this study, two different carrier gases were used; however, it was found that flow rate affected the morphology (density and diameter) of the CNTs alike. It should be noted that higher flow may reduce the reaction temperature. During using SEM, catalyst particle size was observed on the periphery of samples, and higher flow rate produced smaller particles. The phenomenon suggests that the catalyst size is strongly related to flow rate, and smaller catalysts result in smaller diameter of the CNTs. Furthermore, higher flow rate may result in lower temperature of substrate. This effect resulting from the change of flow rate may also cause the morphology of CNTs grown on silicon substrate.



(a) 15 sccm

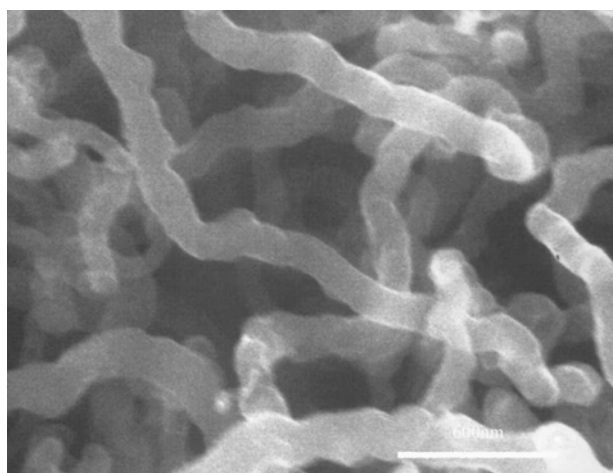


(b) 45 sccm

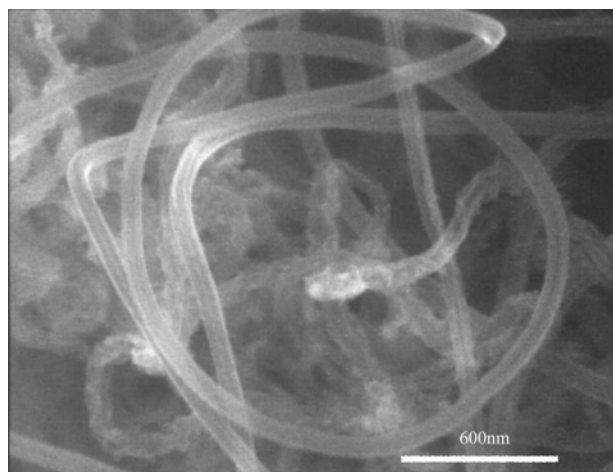


(c) 75 sccm

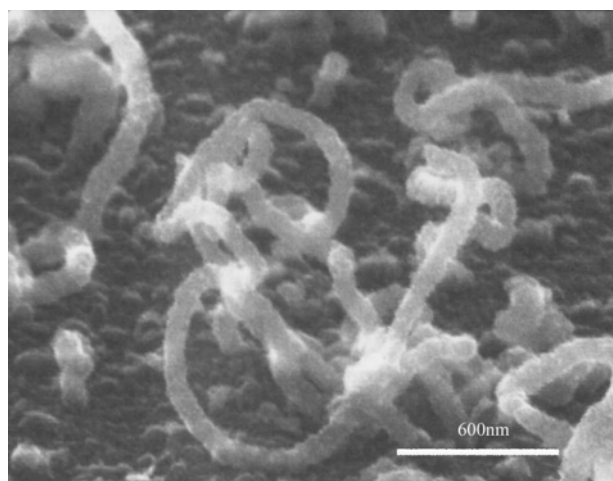
Fig. 24. SEM images of CNTs on silicon, obtained with CO₂ carrier gas of various flow rate; (a) 15 sccm, (b) 45 sccm, and (c) 75 sccm.



(a) 15 sccm



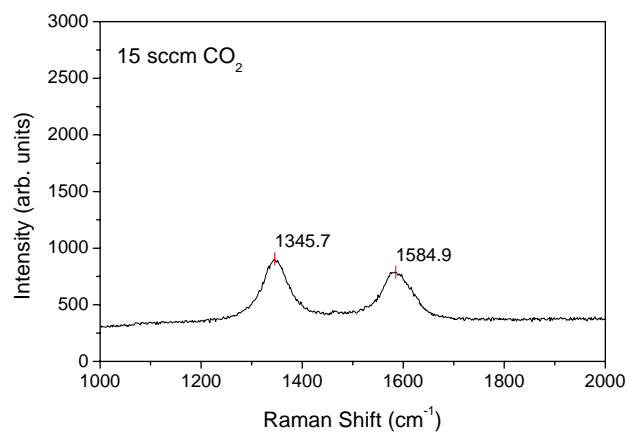
(b) 45 sccm



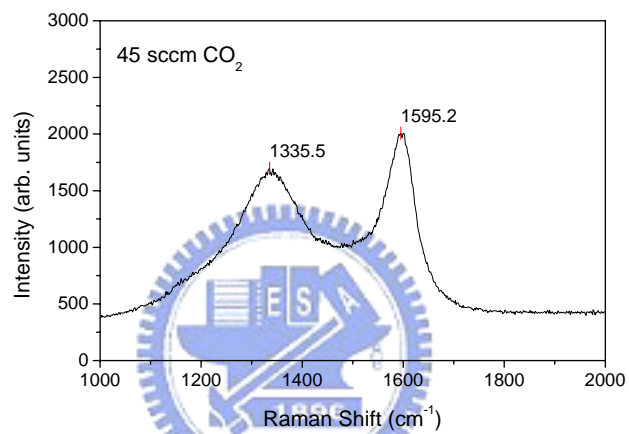
(c) 75 sccm

Fig. 25. SEM images of CNTs on silicon, obtained with Ar carrier gas of various flow rate; (a) 15 sccm, (b) 45 sccm, and (c) 75 sccm.

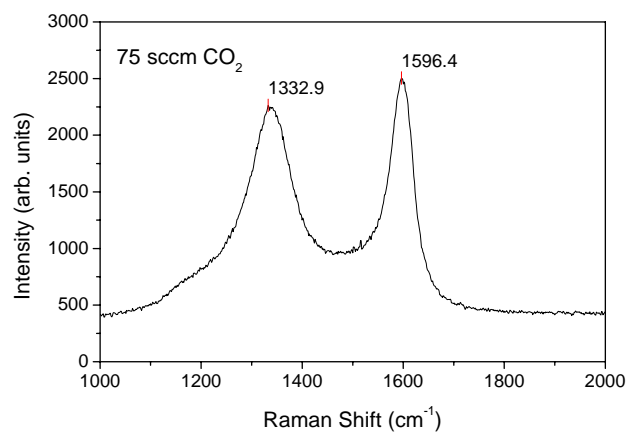
A micro-Raman spectroscopy determines the microstructure and quality of the carbon materials. Figures 26 and 27 display the Raman spectra of the CNTs grown with various carrier gases, CO₂ and Ar. All of them have two sharp peaks located at around 1350 cm⁻¹ and 1581 cm⁻¹. The first-order Raman spectrum of the CNTs shows strong, sharp peaks at 1581 cm⁻¹ (G-line) and 1350 cm⁻¹ (D-line). The peaks suggest that the CNTs are characteristic of microcrystalline graphite. The relative intensities of the two peaks depend on the type of graphitic material. Typically, the intensity of the 1350cm⁻¹ peak increases as (i) the amount of unorganized carbon in the samples increases and (ii) the graphite crystal size decreases. Figures 26 and 27 present the main features of the spectra, agreeing with the observations of other groups [25,157]. The comparable intensities of the G and D lines imply a high density of structural defects [158] in the curved graphene sheets. The SEM and TEM images of the CNTs reveal that the CNTs contain carbon nanoparticles. The appearance of the strong D line can be interpreted as the large amount of crystalline domains on the nanometer scale, increased by the surfaces of the tubes [157]. Thus, in this study, CNTs obtained with higher CO₂ or Ar flow rate have higher quality of microcrystalline graphite.



(a)

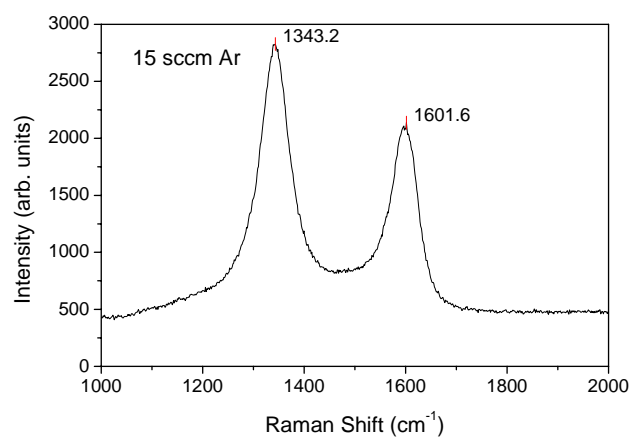


(b)

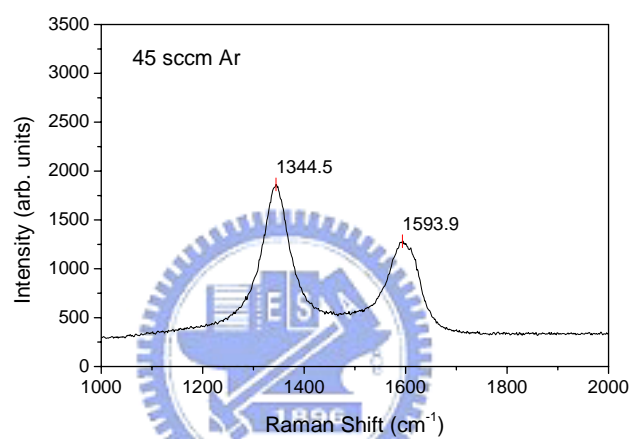


(c)

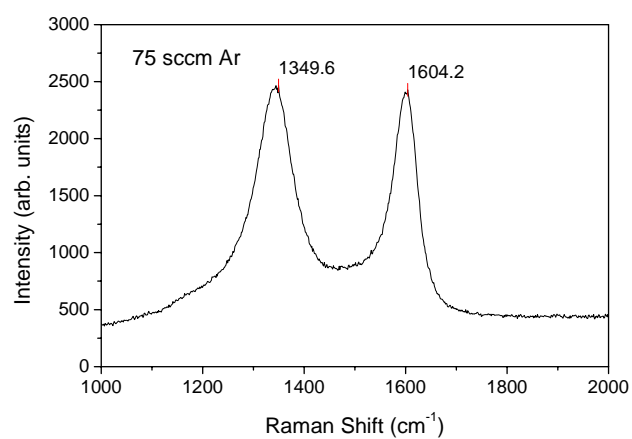
Fig. 26. Micro-Raman spectra of the CNTs grown on the silicon wafer, obtained with CO₂ carrier gas of various flow rate; (a) 15 sccm, (b) 45 sccm, and (c) 75 sccm.



(a)



(b)



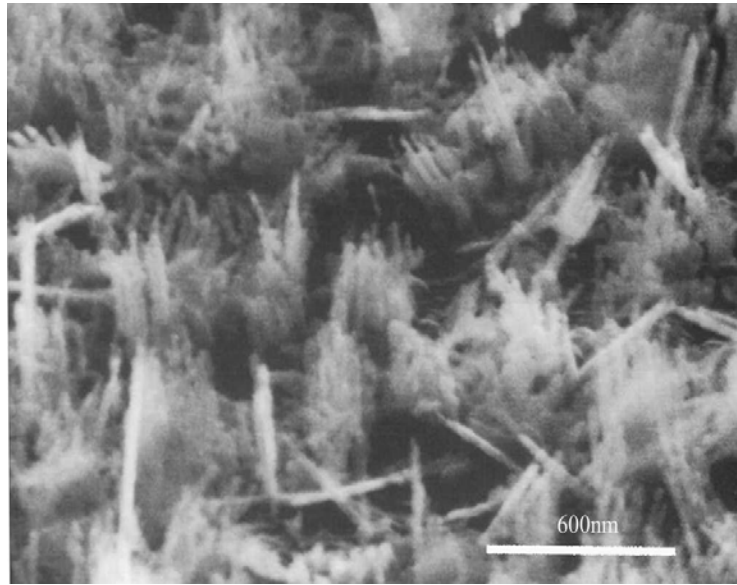
(c)

Fig. 27. Micro-Raman spectra of the CNTs grown on the silicon wafer, obtained with Ar carrier gas of various flow rate; (a) 15 sccm, (b) 45 sccm, and (c) 75 sccm.

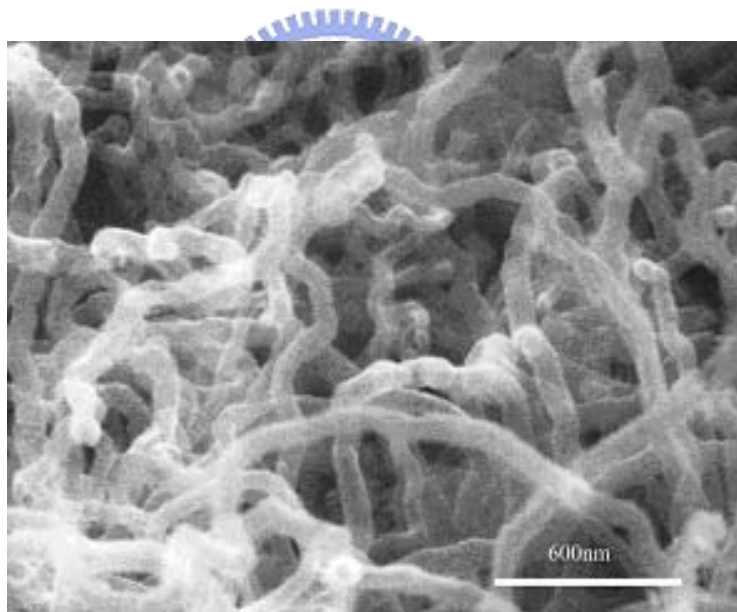
4.1.4 Effect of Carrier Gas Flow Direction on Growth of CNTs

In this study, two carrier gas flow directions were used. CO₂ carrier gas, fixed at 15 sccm flowed vertically or horizontally toward to the substrate by adjusting the nozzle position. After deposition, each sample was first visually examined. The surface of the sample near the bottom of the coiled Fe-Cr wire was the blackest. The location of the CNTs on the sample was examined using SEM. The images reveal that most CNTs were near the bottom of the coiled Fe-Cr wire. Figure 28(a) displays the SEM image of these CNTs. These CNTs were produced when CO₂ carrier gas flowed horizontally to the substrate. Bundles of CNTs are observed on the center of the substrate. The CNTs have a high-aspect-ratio, implying good field emission characteristics. Figure 28(b) shows SEM image of nanotubes obtained using CO₂ carrier gas which flowed vertically toward to the substrate. A fixed CO₂ flow rate of 15 sccm yielded two completely different morphologies. Figure 28(b) shows a random tube network that consists of numerous curved tubes was formed; the tubes are 60-80 nm in diameter and a few tens of microns long.

The first-order Raman spectrum of the both samples, as shown in Fig. 29, show strong, sharp peaks at 1581 cm⁻¹ (G-line) and 1350 cm⁻¹ (D-line). The peaks suggest that both samples are characteristic of microcrystalline graphite.

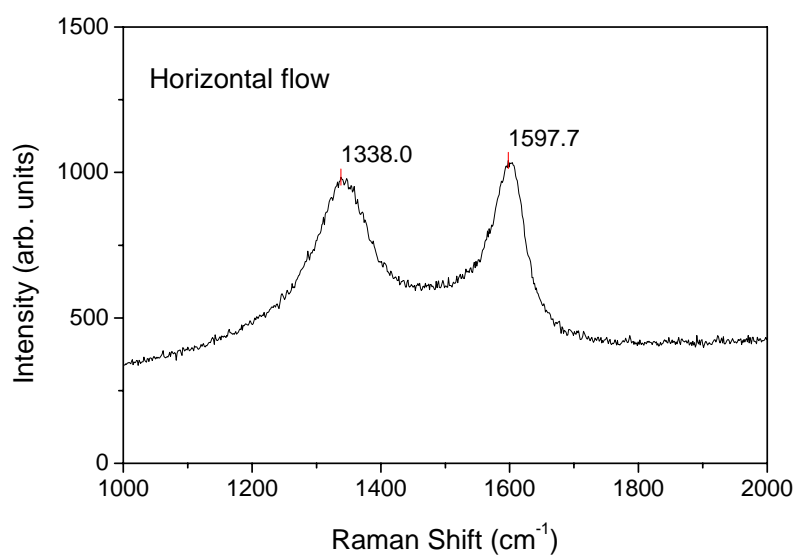


(a) Horizontal flow

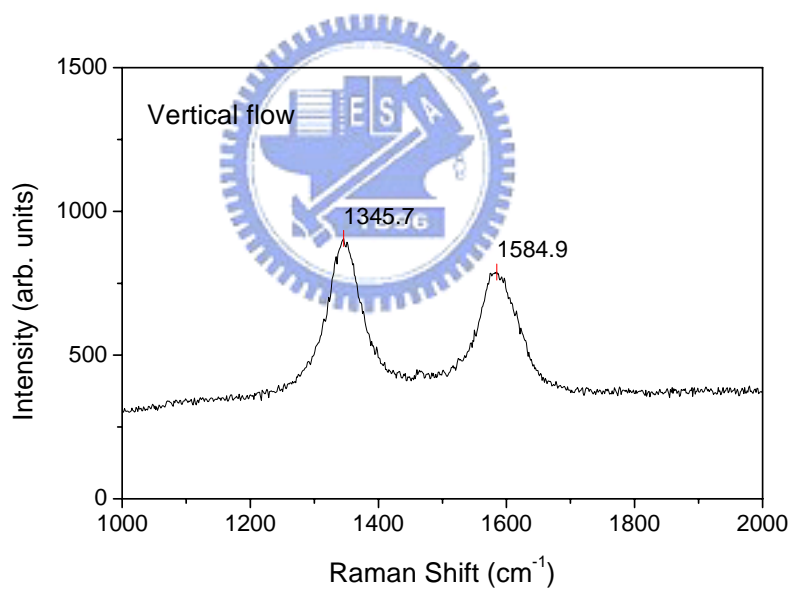


(b) Vertical flow

Fig. 28. SEM images of CNTs on silicon samples. (a) is obtained with CO₂ carrier gas that flows horizontally, and (b) is obtained with CO₂ carrier gas that flows vertically, in this experiment, CO₂ flow rate is constant on 15 sccm.



(a)



(b)

Fig. 29. Micro-Raman spectra of CNTs on silicon samples. (a) is obtained with CO_2 carrier gas that flows horizontally, and (b) is obtained with CO_2 carrier gas that flows vertically.

Figure 30 shows a representative TEM micrograph of the nanotubes obtained with CO₂ carrier gas that flows horizontally. Images show that these tubes are aligned multiwalled CNTs. The darker nanotube walls indicate that the nanotubes are multiwalled and hollow rather than solid fibers. The arrow 1 indicates the wall, and the arrow 2 indicates some defective graphitic sheets at the surface of wall. The CNT have inner diameters of ~ 2 nm and outer diameter of ~10 nm.

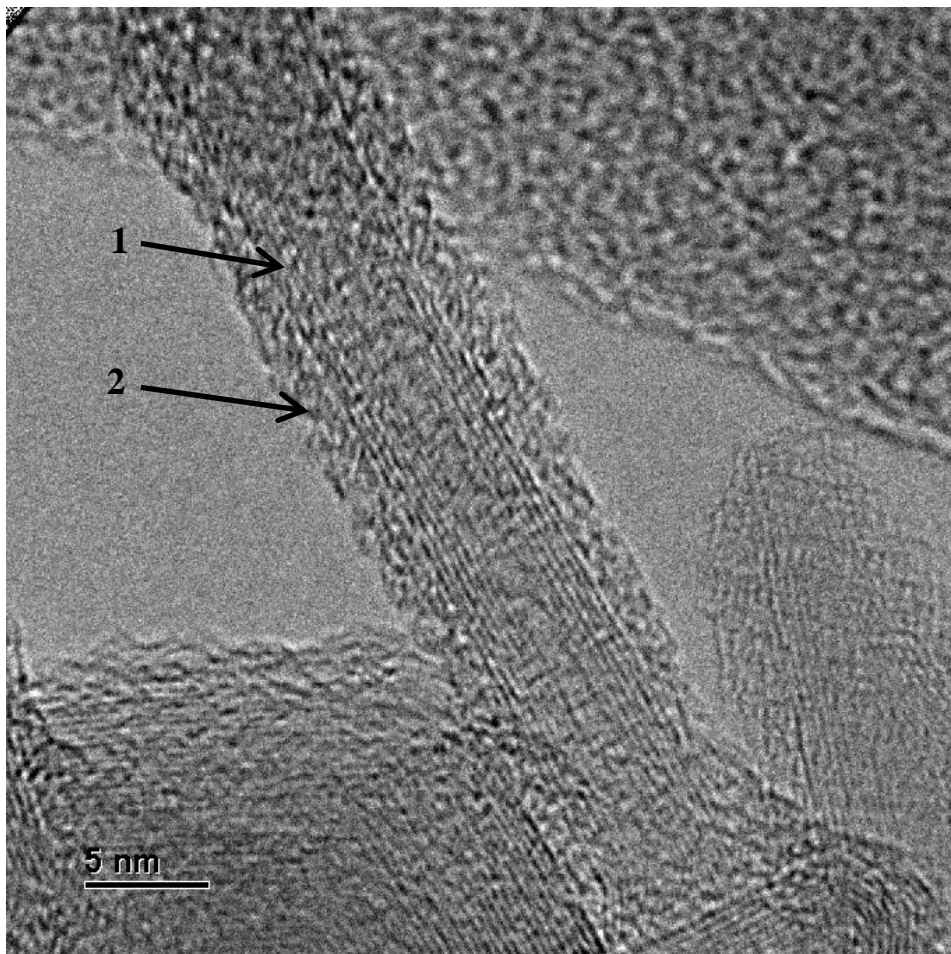
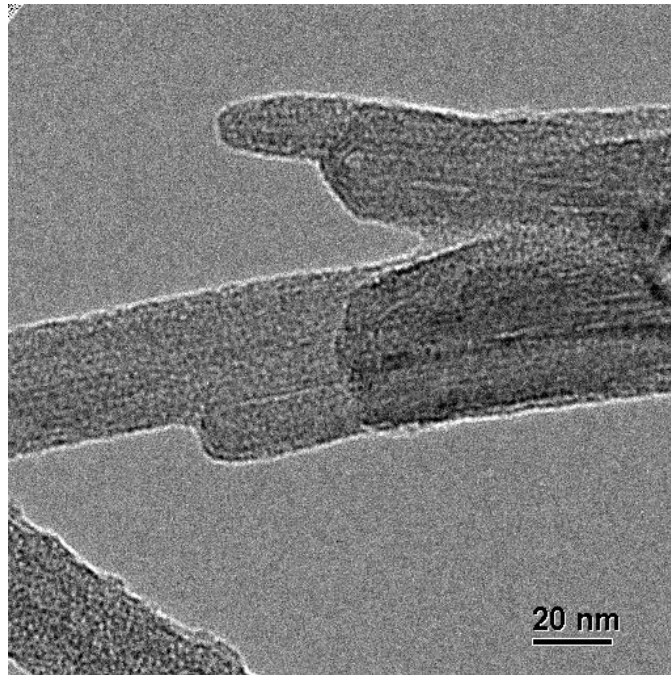


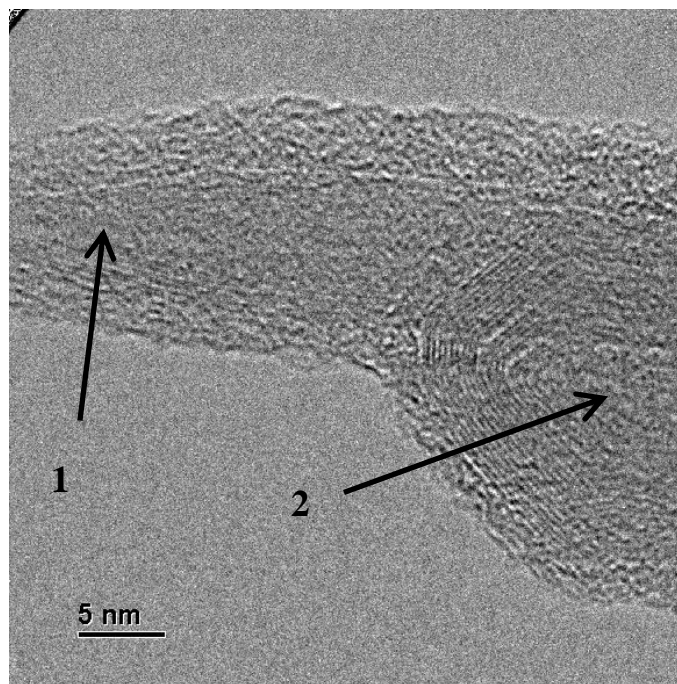
Fig. 30. TEM image of CNT, obtained with CO₂ carrier gas that flows horizontally. The arrows 1 indicates the aligned wall of CNT, and arrows 2 indicates the defective graphitic sheets.

Figure 31 shows TEM images of aligned CNTs grown exhibit no bamboo-like structure. The TEM images reveal the closed tip without any encapsulated metal particles (see arrows 1). It was reported [124] that the smaller average nanotube diameter is directly related to the generation of smaller metal clusters. First, a lower metal concentration in the vapor phase will limit the ability of the metal atoms to agglomerate into large clusters, leading to the formation of smaller metal clusters. In our experiment, it is more likely that metal atoms arrive at the substrate in the vertically flow. Therefore, large clusters formed in such way similar to a higher metal concentration in the vapor phase. Second, it is possible that the properties and temperature of the substrate will also influence the metal particle size. The selection of a substrate on which the metal is more mobile, and/or increasing the substrate temperature, will enhance the processes of nucleation and growth. This will lead to the formation of larger size particles and hence larger diameter nanotubes [125], ultimately affecting a transition to the growth of filaments rather than MWCNTs. However, the properties and temperature of the substrate were constant in our study. Therefore, we supposed that flow direction should change the distribution and particle size of catalysts which originated from filament on the silicon sample.

Under both grow conditions; the temperature of samples was almost the same ($\sim 700\text{ }^{\circ}\text{C}$). Therefore, aligned CNT with a diameter of 10 nm can be grown using this HWCVD method by just adjusting the direction of flow of the carrier gas.



(a)



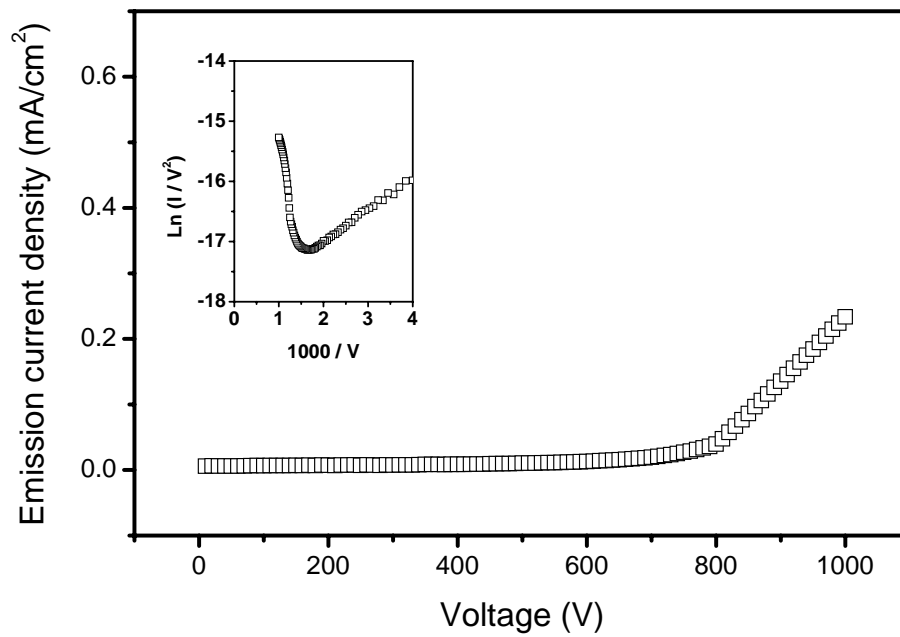
(b)

Fig. 31. TEM images of aligned CNTs grown exhibit no bamboo-like structure; (a) scale bar is 20 nm, and (b) scale bar is 5 nm. The arrows 1 and 2 indicate the closed tips with no encapsulated metal particle.

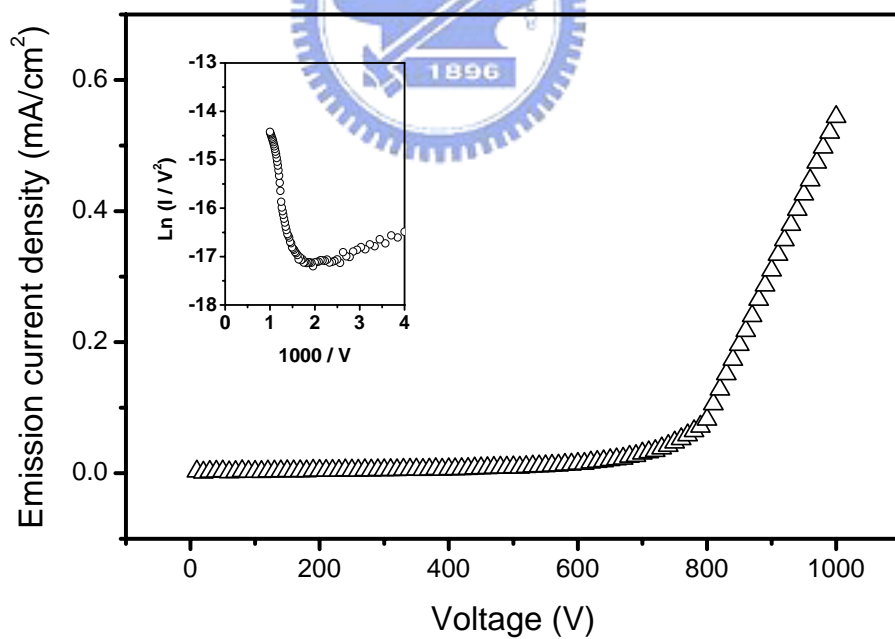
4.1.5 Field Emission Properties

Figure 32 displays the electron-emitting characteristics of the random curved and aligned CNTs. The emission current density of curved CNTs at an applied voltage of 1000 V (2 V/ μm) was 0.234 mA/ cm^2 . The macroscopic turn-on field, which is the field needed to extract current density of 10 $\mu\text{A}/\text{cm}^2$, was 1.34 V/ μm . The emission current density of aligned CNTs was 0.54 mA/ cm^2 . The macroscopic turn-on field was 1.1 V/ μm . Bonard et al. reported [159] that a comparison among film field emitters is pertinent only if the field emission measurements, especially the inter-electrode distance and geometry, were taken under the same experimental conditions. In this study, it could be proved that aligned CNTs possessed better electron-emitting characteristics than those of curved CNTs. Furthermore, the field enhancement factor, β , of aligned CNTs grown here is to be extracted using a commonly used method.

Fowler and Nordheim in 1928 proposed the first model of field emission from a solid [130]. The F-N model states that the relationship between the emitted current in the local electric field F and the work function ϕ is $I \propto (F^2 / \phi) \exp(-B\phi^{3/2} / F)$, with $B = 6.83 \times 10^9$ [$\text{VeV}^{-3/2}\text{m}^{-1}$]. The local electric field F is not simply V/d , which is the macroscopic field obtained with an applied voltage V between two electrodes separated by a distance d . Rather, F is, in most cases, larger by an enhancement factor β , which reflects the ability of the emitter to amplify the field. β is determined mostly by the geometrical shape of the emitter, and the field at the emitter surface is frequently expressed as $F = \beta E = \beta V/d$, where $E = V/d$ is the macroscopic field. Moreover, the literature includes arguments based on values of β that have been determined from the shape of the emitter, and especially from its radius of curvature at the tip, R_{tip} . The most basic approximation is $F \approx V/(k \cdot R_{tip})$, where k is a constant that depends on the geometry and is taken to be equal to 5 for an infinitely long cylindrical emitter [160]. From the above definition and approximation for F , $\beta = d/(5 \cdot R_{tip})$ is obtained. Thus $R_{tip} = 5$ nm yields $\beta = 20000$.



(a)



(b)

Fig. 32. Emission current density against applied voltage and the F-N plot of (a) random curved CNTs, and (b) aligned CNTs.